

Cite this: *Nanoscale*, 2019, **11**, 4337

## Silvered conical-bottom 96-well plates: enhanced low volume detection and the metal-enhanced fluorescence volume/ratio effect<sup>†</sup>

Rachael Knoblauch and Chris D. Geddes\*

Many diagnostic fluorescence assays are limited by sensitivity (signal/noise) and minimum sample volume requirements. Herein we report a new, silvered conical-bottom 96-well plate platform used to increase the detectability from very small volumes of micromolar concentrations of fluorophores. This technology employs the principles of metal-enhanced fluorescence (MEF), which is the process by which fluorescence emission is amplified in the near-field of plasmonic nanoparticles. By combining the MEF effect with the advantages of a small volume conical well, we report and characterize detectable emission from fluorescent solutions down to 3 microliters in volume. We report enhancement factors for fluorescein and Rhodamine 6G and correlate these factors to the synchronous scattering spectra of the silvered conical wells. Subsequently, we determine corrected enhancement factors and discuss enhancement in terms of the MEF volume ratio effect and per mole of enhanced fluorophore. The research reported herein sets the foundation for future development of even more powerful MEF-based diagnostic assays.

Received 18th December 2018,

Accepted 18th February 2019

DOI: 10.1039/c8nr10220a

rsc.li/nanoscale

## 1. Introduction

Biomedical diagnostics, and in particular immunodiagnostics, has heavily employed fluorescence-based assays to detect species of interest in biological media; these assays, however, are limited by sensitivity, large sample volume requirements, unwanted background fluorescence, and complex assay preparation procedures. To overcome some of these limitations, metal-enhanced fluorescence (MEF) has become an increasingly important and now commercially available technology. MEF is the phenomenon by which the emission intensity of a fluorophore is amplified in the near-field of plasmonic metal nanomaterials. This process is thought to occur as a function of two mechanisms, enhanced absorption and enhanced emission, and occurs when fluorophores couple to metal-surface plasmons to radiate quanta.<sup>1</sup> This unified plasmon-fluorophore model describes the many unique spectroscopic characteristics of MEF reported previously by our lab and others, one of which is the distance-dependence of enhancement.<sup>1–3</sup> Specifically, only fluorophores (dipoles) in the near-field of the plasmonic material can couple to plasmons, leading to a

larger magnitude MEF effect as more fluorophores are brought into close proximity. Numerous fluorescence assays have been developed applying this principle of distance-dependent MEF response to circumvent the limitations of current assays on blank 96-well plates, which include lengthy incubation times and washing steps or complex probe design.<sup>4–7</sup> In the design of MEF-based assays, however, changes in enhancement factor or simply signal intensity can be monitored to detect and quantify a species of interest.<sup>8,9</sup> MEF-based assays have been used to gain sensitivity at sub-picomolar concentrations, and thus expand the detection power of current technologies for even more sensitive diagnostics.<sup>9–11</sup> To date, the most pervasively used MEF platform is on “2D” substrates, including flat-bottomed 96-well plates;<sup>12</sup> these well plates are already standard in high-throughput assay development, and thus their modification for MEF has been a logical extension of current technologies. In fact, silvered 96-well plates for enhanced emission detection are available today from Ursa BioScience (<http://www.ursabioscience.com>). Using this configuration, however, has not improved detection for samples of very limited available volume. In order to achieve effective and consistent detection by plate readers, the entire base of a sample well must be filled and covered. This leads to a minimum sample volume of approximately 80 µL for standard, flat-bottom 96-well plates (Fig. S1†), which can be limiting if the amount of available sample is below this volume minimum. Herein we report the fabrication and characterization of new silvered conical-bottom 96-well plates for potential use in MEF

Institute of Fluorescence and the Department of Chemistry and Biochemistry,  
University of Maryland Baltimore County, 701 E Pratt Street, Baltimore, Maryland,  
21202, USA. E-mail: geddes@umbc.edu; Fax: +1(410) 576-5722;

Tel: +1(410) 576-5723

† Electronic supplementary information (ESI) available. See DOI: 10.1039/c8nr10220a

assays. Changing the shape of the well lowers the minimum detectable volume by approximately 25-fold, and thus sets the precedent for the development of significantly more powerful MEF-based assays.

## 2. Materials and methods

### 2.1. Conical well fabrication

Conical-bottom polypropylene 96-well plates were purchased from Fisher Scientific (Nunc<sup>TM</sup>, conical) along with silver nitrate. Sodium hydroxide, ammonium hydroxide, glucose, fluorescein sodium salt, and Rhodamine 6G were purchased from Sigma Aldrich. While the plates were plasma cleaned, solutions for silver deposition (0.83% silver nitrate, 5% sodium hydroxide, 28% ammonium hydroxide, and 4.8% glucose) were prepared in deionized water and cooled to and stored at approximately 10 °C. When ready for use, solutions were removed from the refrigerator and kept on ice during the silver nano-polishing process. A solution of 20 mL silver nitrate, 98 µL sodium hydroxide, 520 µL ammonium hydroxide, and 5 mL glucose was prepared and loaded into the wells at 240 µL volumes using a multichannel pipette (8 channels) to speed up the process. The resulting plate and solution were then incubated on a heating mantle (VWR) with an added aluminum mold at 48 °C for two minutes, followed by a two-minute incubation in a freezer (~−20 °C), and a secondary two-minute incubation in the heat block to form the initial silver layer. This custom heating block was machined from aluminum to provide an exact fit to the underside of the black conical well plates, such that homogeneous heating occurred from the mantle (Fig. 1). The remaining solution was dis-

carded, and the wells were rinsed in triplicate with deionized water and air-dried. The same solution was prepared again and loaded, with a heating incubation period of three minutes before being discarded and rinsed to form layer 1.

This three-minute incubation procedure was repeated with new solution for 13 additional layers, to generate wells with 3 to 14 silvered layers for subsequent experiments (Fig. S2†).

### 2.2. Spectral properties and metal-enhanced fluorescence measurements

Following fabrication, the wells were air-dried at room temperature and intensity measurements were collected using a Varian Cary Eclipse Fluorescence Spectrophotometer equipped with a plate reader for fluorescein and Rhodamine 6G, at varying volumes and concentrations indicated throughout the manuscript. Synchronous scattering spectra, or spectra collected when the wavelength of excitation is equal to the detected emission wavelength ( $\lambda_{\text{ex}} = \lambda_{\text{em}}$ ), were also gathered using the Varian spectrophotometer. Red shifts were determined using the emission wavelength corresponding to maximum intensity, and full width half maxima (FWHM) were calculated using these same intensity values.

### 2.3. Calculation of metal-enhancement values

Metal-enhancement factors (MEF) at set wavelengths were calculated by dividing the fluorescence intensity of the fluorophore in silvered wells by the intensity of those detected on plastic wells at the wavelength of interest. In addition, these MEF values, determined by the raw data, were subsequently corrected at each concentration for the various sample volumes; this was done by incorporating the percent of solution within the defined MEF region (%MEF) into the enhancement determination to yield a corrected MEF value, labeled  $\text{MEF}_C$ . This calculation is summarized in eqn (1), where  $V_{\text{MEF}}$  is the volume of fluorophore in the MEF region and  $V_{\text{sample}}$  is the total volume of solution analyzed.

$$\% \text{MEF} = \frac{V_{\text{MEF}}}{V_{\text{sample}}} \times 100 \quad (1)$$

Finally, this value was calculated in terms of moles in the MEF region ( $\text{MEF}_C \text{ mol}^{-1}$ ). For more detail regarding the correction calculations, refer to the ESI sections S2.3.1 and S2.3.2.† These describe the method by which the well dimensions were modeled (Schemes S1 and S2, Table S1†), with subsequent reported values for %MEF at varying samples volumes (Table S2†).

## 3. Results and discussion

### 3.1. Analysis of the synchronous scattering spectra

As reported previously by our lab, the relative magnitude of MEF at different wavelengths frequently can be predicted by examining the synchronous scattering spectrum of the plasmonic material.<sup>13</sup> Subsequently, we analyzed the scattering characteristics of the wells after each silver layer was added as shown in Fig. 2. By doing so, trends in enhancement could be



**Fig. 1** Conical well plate aluminum mold (top) and heating block (bottom) used for silver deposition.

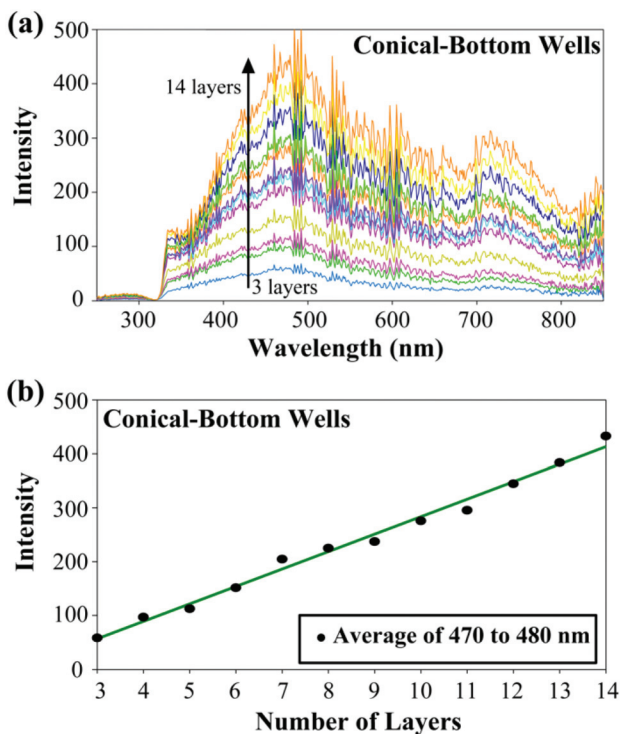


**Fig. 2** Synchronous scattering spectral data for silver-coated conical-bottom wells for multiple layers of silver deposition. (a) Synchronous scattering spectra for wells over  $\lambda_{\text{ex/em}} = 250 \text{ nm} - 850 \text{ nm}$ . (b) Averaged intensities at peak scattering wavelengths plotted against number of silvered layers.

predicted for the wells after each deposition cycle. MEF has been shown to occur favorably at wavelengths where the scattering component dominates the extinction spectrum of the plasmonic material;<sup>14</sup> thus it is reasonable, and in fact experimentally verified, to predict that MEF will be most pronounced for systems with highly scattering plasmonic nanomaterials, as compared to those substrates with extinction spectra dominated by absorption. MEF is further improved when metals are coupled with fluorophores that have specific spectral properties (*i.e.* excitation and emission wavelength) that overlap favorably with optimal scattering wavelengths.<sup>3,15</sup> As shown by Fig. 2, with the incorporation of additional silver layers there is a corresponding scattering intensity increase, demonstrating a linear relationship. These data not only confirm the successful layering of silver per the procedure, but also indicate the possibility of higher MEF factors for fluorophores in the multi-layered wells. The silvered wells exhibit peak scattering properties at emission wavelengths of 470 to 480 nm, although scattering is still effective across the visible range.

In addition, the spectra collected do not vary significantly in shape. As such, scattering properties of the silver could be considered to trend linearly across the entire detected range. Based on these data, it is predicted that enhancement for both fluorophores discussed herein will be maximal for the 14-layer substrates. This observation will be discussed in more detail in subsequent sections.

### 3.2. Correlation of MEF to the synchronous scattering spectra

Fluorescein sodium salt ( $\lambda_{\text{ex}} = 490 \text{ nm}$ ,  $\lambda_{\text{em,max}} = 518 \text{ nm}$ ) and Rhodamine 6G ( $\lambda_{\text{ex}} = 506 \text{ nm}$ ,  $\lambda_{\text{em,max}} = 535.97 \text{ nm}$ ) are two commonly used fluorophores for fluorescence-based assays, with excitation and emission properties that overlap favorably with those of the silver nanomaterial used in this study. As such, these fluorophores were chosen to analyze the effective detection of MEF from conical-bottom wells. A  $100 \mu\text{M}$  solution of fluorescein sodium salt was added to the wells and fluorescence intensity detected at  $490 \text{ nm}$  excitation. As indicated in Fig. 3, a volume range of 3 to  $80 \mu\text{L}$  was tested. Whereas this volume range would be largely undetectable on a flat-bottomed well platform, a clear signal was apparent for the conical wells at  $3 \mu\text{L}$  volumes, even for the uncoated plastic plate (Fig. 3b).

Enhancement from proximity to silver is clearly shown in the emission spectra for all volumes (3, 4, 5, 20, 50, and  $80 \mu\text{L}$ ) for  $100 \mu\text{M}$  fluorescein, shown in Fig. 3 and ESI Fig. S3 and S4.† Additionally,  $10 \mu\text{M}$  fluorescein was analyzed and simi-

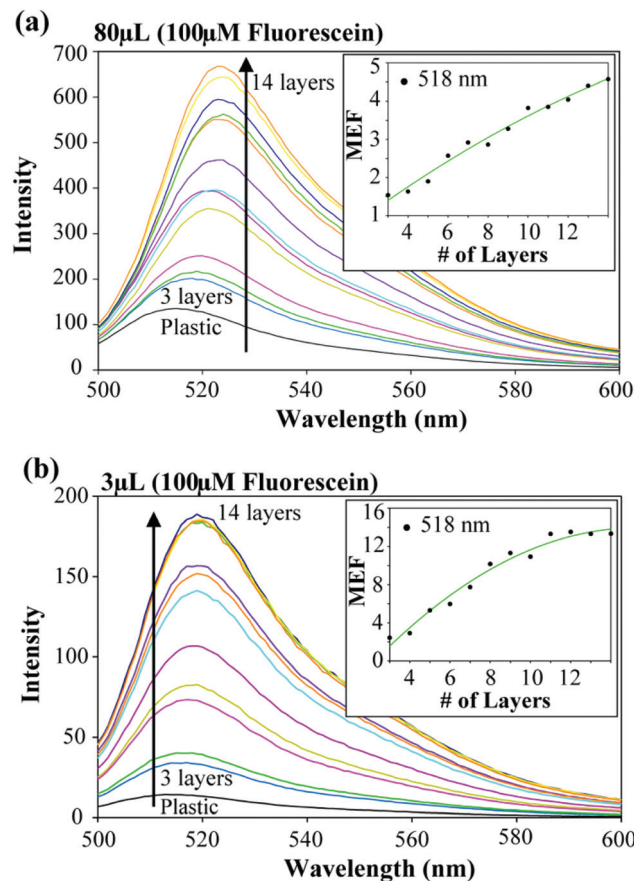


**Fig. 3** Comparison of metal-enhanced fluorescence from emission spectra ( $\lambda_{\text{ex}} = 490 \text{ nm}$ ) of  $100 \mu\text{M}$  fluorescein in conical-bottom wells with various silvered layers for sample volumes of (a)  $80 \mu\text{L}$  and (b)  $3 \mu\text{L}$ . Insets display metal-enhancement factors (MEF) calculated at emission wavelength =  $518 \text{ nm}$  as a function of number of silvered layers. Enhancement factors are calculated as emission from the silvered wells divided by that from the control sample, *i.e.* the plastic wells.

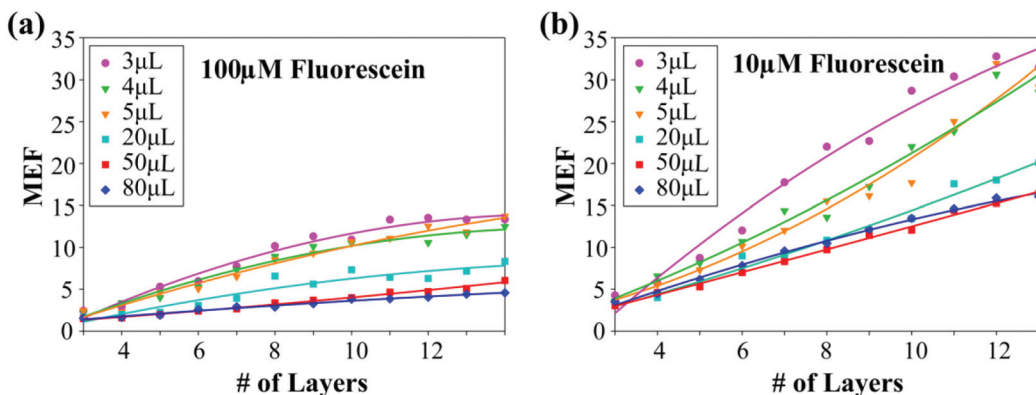


**Fig. 4** Metal-enhanced fluorescence responses of fluorescein in conical wells with varying silvered layers for fluorescein concentrations of (a) 100  $\mu\text{M}$  and (b) 10  $\mu\text{M}$ . Metal-enhancement factors (MEF) were calculated at  $\lambda = 518 \text{ nm}$ .

larly demonstrates enhancement on silvered conical wells (Fig. 4). For all volumes tested at each concentration, the enhancement factor increases with the number of silvered layers as predicted by the synchronous scattering spectra, confirming the relationship between MEF and scattering properties of the plasmonic material.

Solutions of Rhodamine 6G were also analyzed as both fluorescein and Rhodamine are xanthene-type fluorophores and therefore share spectral similarities. Rhodamine, however, exhibits a slightly red-shifted emission. Analogous to fluorescein, solutions of Rhodamine 6G demonstrated significant enhancement when placed in the silvered conical wells (Fig. 5). MEF also increased as the number of silvered layers increased, indicating excellent correlation with the synchronous scattering spectra. This correlation was examined for 100, 10, and  $\sim 1 \mu\text{M}$  solutions of Rhodamine 6G, at volumes of 3, 4, 5, 20, and 50  $\mu\text{L}$  (Fig. 6 and S5–S8†). 1 and 2  $\mu\text{L}$  volumes were also analyzed, although background scattering from the silvered substrate cause significant spectral distortion and subsequently were not considered.

Upon examination of MEF from different sample volumes at constant concentrations, Fig. 4 and 6 exhibit an apparent volume dependence of MEF with larger values reported for smaller volumes. This is likely due to the MEF volume ratio effect, which will be discussed in detail in section 3.4. It is noteworthy from these data, however, that enhancement increases are observed for both fluorescein and Rhodamine for the silvered conical wells as number of silvered layers, and therefore synchronous scattering intensity, is increased. The growing body of evidence for synchronous spectral correlation to MEF magnitude thereby sets the foundation for better fluorophore/nanoparticle selection in the development of assays using the conical well platform.

### 3.3. Spectral characteristics of enhanced fluorophore emission

As shown by Fig. 3 and 5, it is interesting to note that the enhanced spectra demonstrate an overall red-shifted emission

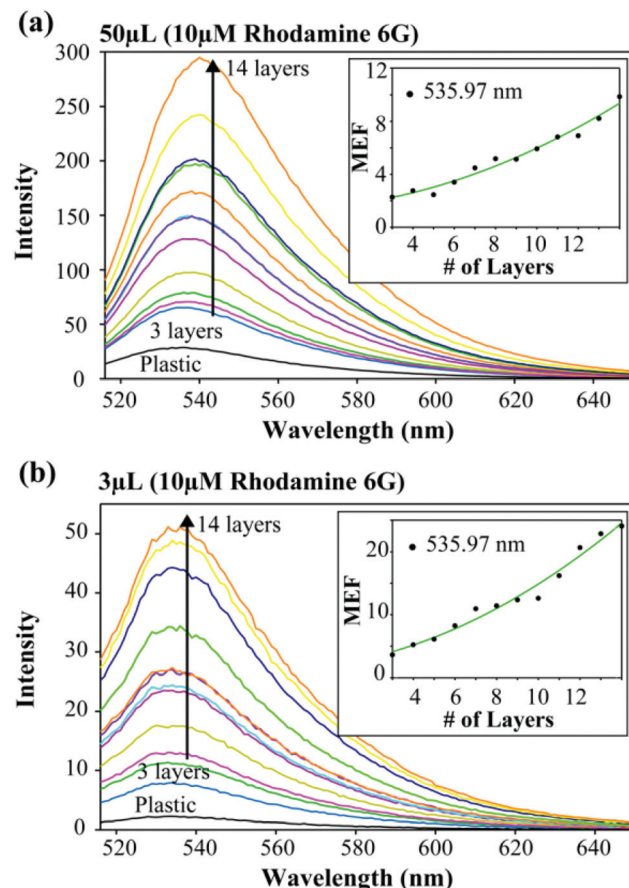


**Fig. 5** Comparison of metal-enhanced fluorescence from emission spectra ( $\lambda_{\text{ex}} = 506 \text{ nm}$ ) of 10  $\mu\text{M}$  Rhodamine 6G in conical bottom wells with various silvered layers, for sample volumes of (a) 50  $\mu\text{L}$  and (b) 3  $\mu\text{L}$ . Insets display metal-enhancement factors (MEF) calculated at emission wavelength = 535.97 nm as a function of number of silvered layers. Enhancement factors are calculated as emission from the silvered wells divided by that from the control sample, i.e. the plastic wells.

when compared to the blank plate (Fig. S9†). This spectral distortion, while not widely reported, has been observed by our group in MEF from other fluorophores.<sup>16,17</sup> Although this

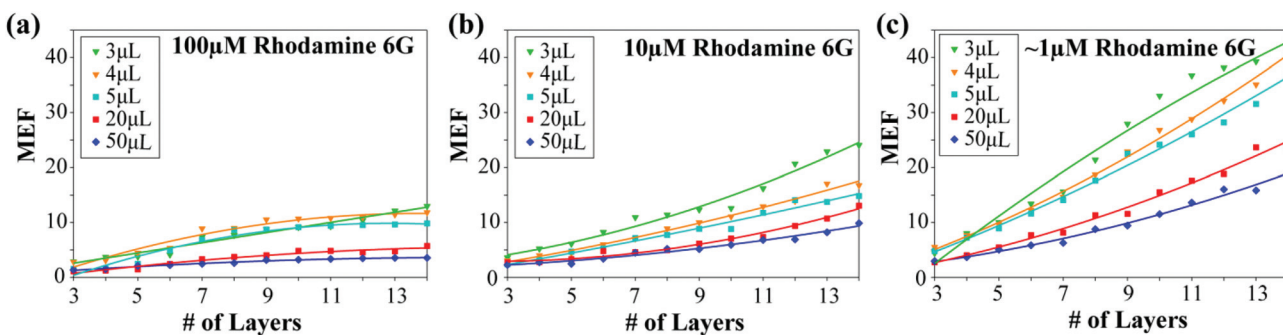


**Fig. 6** Metal-enhanced fluorescence responses of Rhodamine 6G in conical wells with varying silvered layers for Rhodamine 6G concentrations of (a) 100  $\mu\text{M}$ , (b) 10  $\mu\text{M}$ , and (c)  $\sim$ 1  $\mu\text{M}$ . Metal-enhancement factors (MEF) were calculated at  $\lambda = 535.97 \text{ nm}$ .

effect is not well understood, it has been postulated to be a consequence of a changing continuum of plasmon energy levels with nanoparticle growth and different rates of plasmonic coupling with fluorophores.<sup>16</sup> It is well known that the localized surface plasmon resonance (LSPR) band of silver nanoparticles will red shift as the particles grow in size.<sup>15,18</sup> If the silver nanoparticles deposited on the conical-bottom wells grow with each layering cycle, one would expect the wells to subsequently absorb and scatter red-shifted wavelengths more efficiently, leading to the observed red-shifted spectra for fluorophores detected in the many-layered silvered wells.

Interestingly, an increase in full width half maximum (FWHM) of the fluorophore emission is observed as more layers of silver are deposited in the wells (Fig. S9†). This increase in FWHM correlates also to the increase in the MEF factor discussed earlier, which is *unexpected* by current MEF theory.<sup>16,17</sup> When considering the enhanced emission component of the MEF mechanism, one would expect that the FWHM should narrow for the plasmon-amplified spectra. This is thought to be due to the faster radiative decay channels (rate) of the coupled system, due to increase in the density of states of the coupled system. As the rate of radiative decay increases, non-radiative decay pathways become less competitive for excited state relaxation. Peak narrowing should become more pronounced as MEF increases; however, broadening occurs rather than narrowing as MEF factors rise for these data. This seemingly inverse observation could suggest heterogeneous nanoparticle growth within the wells. Such growth would yield a distribution of different-sized silver particles over the well surface area and would thus permit plasmonic coupling to varying energetic states, some resulting in quicker radiative pathways and others much longer. Under these conditions and detection parameters, each different coupled emission signal would not be distinctly isolated and would therefore contribute to the overall broader emission spectrum. With heterogenous nanoparticle growth, greater red shifts and FWHM values may also be predicted for higher sample volumes, as fluorophores in solution would couple with a larger area—and possibly a larger distribution—of nanoparticles. This predicted spectral distortion is observed, as shown in ESI Fig. S9.†

### 3.4. Analysis of corrected MEF values

As mentioned previously, Fig. 4 and 6 seem to exhibit higher MEF values for those samples detected at lower volumes. This trend is observed for both fluorophores, at each concentration tested. Detected MEF, however, is highly dependent upon sample volume, as only a small portion of the solution is within the  $\sim$ 50 nm range that will result in coupling to the plasmonic material. In fact, for the system described herein, <0.1% of the solution in the conical wells occupies this region, termed the MEF region volume (Table S2†). MEF values, however, are calculated proportional to the total emission intensity of the blank well fluorophore; therefore, MEF values underestimate true enhancement by assuming 100% of the solution couples and may contribute to signal amplification. As such, samples with lower volumes will have a greater contribution of the MEF region to the total volume, resulting in higher calculated MEF values.

This can be considered as the MEF volume ratio effect, and therefore inherent error is included when one attempts to compare enhancement across sample volumes when MEF is calculated in this manner. As such, corrected MEF ( $\text{MEF}_c$ ) values were calculated and are summarized for fluorescein in Fig. 7. These data indicate that when volume is corrected for in the MEF calculation, there is actually no significant difference between enhancements from different sample volumes at constant concentration. This was also observed for Rhodamine at 10  $\mu\text{M}$ , although deviation from this trend was detected for both the 100 and  $\sim$ 1  $\mu\text{M}$  concentrations (Fig. S10†). For the former, inter-filtering effects at this higher concentration could limit detected enhancement, leading to the plateau in  $\text{MEF}_c$  values as observed in Fig. S10a.† At the  $\sim$ 1  $\mu\text{M}$  concentration, significant contribution from background scattering may result in a poor signal to noise ratio that further distorts upon correction.

The corrected values were then calculated per mole of fluorophore within the MEF region. The values calculated are reported for fluorescein in Fig. 8, with those for Rhodamine included in ESI Fig. S11.† Interestingly, samples with lower analysis volumes seem to yield higher enhancement per mole than those detected at higher sample volumes (Fig. 8a and b);

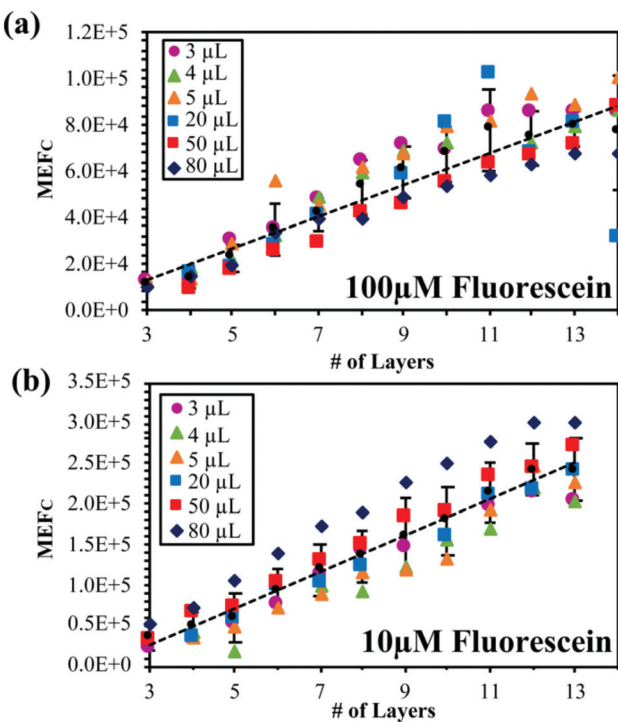


**Fig. 7** Corrected metal-enhanced fluorescence responses of fluorescein in conical wells with varying silvered layers for fluorescein concentrations of (a) 100  $\mu\text{M}$  and (b) 10  $\mu\text{M}$ . Corrected metal-enhancement factors ( $\text{MEF}_C$ ) were calculated from corresponding MEF values. Trendlines are from series averages (black circles).

however, when these trends are normalized, the increase in enhancement per silvered layer is comparable between sample volumes (Fig. 8b and c). Deviations in the data for Rhodamine can be attributed also to the errors discussed previously for  $\text{MEF}_C$  values. The overall comparable increase in enhancement with increased layering indicates that despite achieving more efficient coupling at lower analysis volumes, the synchronous scattering spectral data is still sufficient to predict trends when it comes to silvered well preparation. The higher  $\text{MEF}_C$  per mole of fluorophore that is observed for smaller volumes in the conical wells could be the result of a variety of factors. Although this is not yet well understood, studies have demonstrated that strong emission enhancement can be exhibited when plasmonic nanomaterials sequester fluorophores into nano-sized or sub-wavelength pores and cavities.<sup>19,20</sup> In fact, it is likely that at the conical apex the electric field generated by the nanoparticles has different distribution than would be observed for a flat-bottomed well,<sup>21</sup> changing the distance-dependence, and subsequently the MEF volume region, of the fluorophore solutions near-to the apex. This would be particularly impactful at lower volumes, where more of the MEF region is dominated by the conical apex volume. This intriguing phenomenon requires further study to understand the nature of plasmonic coupling and MEF in a nanometer-scale conical configuration.

From the data described previously, there also appears to be a concentration dependence for  $\text{MEF}_C$  and  $\text{MEF}_C \text{ mol}^{-1}$  values, with lower concentrations resulting in higher detected

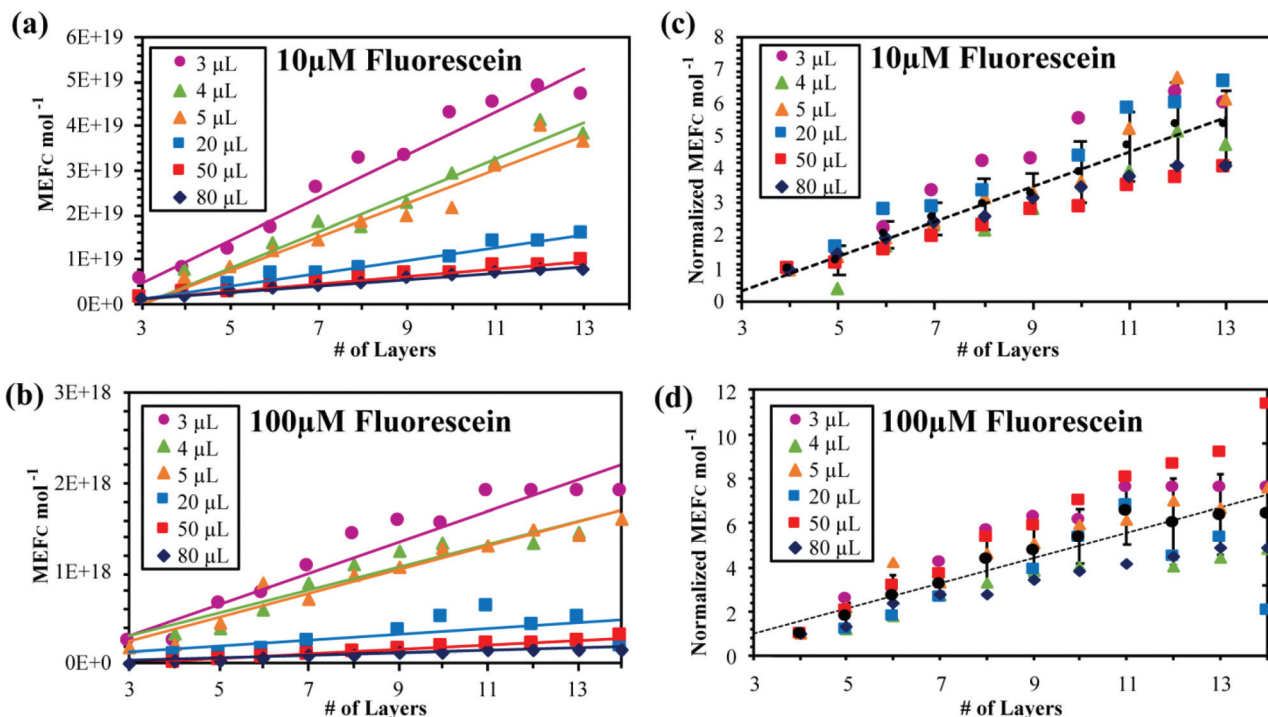


**Fig. 8** Corrected metal-enhanced fluorescence responses (calculated per mole,  $\text{MEF}_C \text{ mol}^{-1}$ ) of fluorescein in conical wells with varying silvered layers for concentrations of (a) 10  $\mu\text{M}$  and (b) 100  $\mu\text{M}$ . Normalized plots are included for concentrations of (c) 10  $\mu\text{M}$  and (d) 100  $\mu\text{M}$ . Trendlines are from series averages (black circles).

enhancement. Rather than being an inherent consequence of the mechanism of MEF, this observation is likely due to a decreased signal to noise ratio for samples with lower concentrations.

Since emission collected in this study was not filtered by polarization prior to detection, the spectra for all samples on silvered wells contain a measure of background scattered wavelengths from silver alone, which contributes to the spectra and therefore the reported values. This effect becomes more pronounced at lower concentrations where the fluorescence signal becomes comparable in intensity to that of background scattering. With the detection of low-concentration, low-volume samples in application, this merely presents a consideration for assay developers that could easily be accounted for during calibration.

## 4. Conclusion

Herein we have reported a new platform for future MEF-based assays that expands the potential for current silver-coated platforms. Although silvered 96-well plates for MEF assays are currently commercially available, this study examines the application of this coating technology to conical wells. While flat-bottomed wells are limited by ~80 microliter detection volumes, herein we observe efficient detection of enhanced spectra down to 3 microliters for the new conical wells. In fact, the enhancement values for these low volumes are surprisingly larger than those at higher volumes, making the conical well plates an even more attractive alternative for detection in assays with limited available sample. Examination of the corrected MEF values reveals that high enhancement for small volumes is likely a consequence of the MEF volume ratio effect. MEF can be further tuned by varying the number of silvered layers, resulting in more significantly enhanced spectra that also demonstrate broadened full width half maxima. This phenomenon indicates not only potential heterogeneous growth of the nanoparticles, but also the possible emission of both faster and slower transitions for the coupled system. The results of our study set the foundation for future assay development on silvered conical-bottom wells, with the aim of achieving even more sensitive diagnostics where previous assay design has been limited by the need for high-volume samples.

## Author contributions

All information reported was written by Rachael Knoblauch and edited by Dr Chris D. Geddes. All experiments were conducted by Dr Chris D. Geddes. Additional data analysis and calculations were completed by Rachael Knoblauch.

## Abbreviations and variables

MEF	Metal-enhanced fluorescence
LSPR	Localized surface plasmon resonance

FWHM	Full width half maximum
%MEF	Percent of solution within the defined MEF region
MEF <sub>C</sub>	Volume-corrected metal enhancement factor
MEF <sub>C</sub> mol <sup>-1</sup>	Volume-corrected metal enhancement factor per mole of fluorophore in MEF region
V <sub>MEF</sub>	Volume of fluorophore solution in MEF region
V <sub>sample</sub>	Total volume of solution analyzed

## Conflicts of interest

There are no conflicts of interest to declare.

## Acknowledgements

The authors acknowledge the Institute of Fluorescence (IoF) as well as the Department of Chemistry and Biochemistry at the University of Maryland Baltimore County (UMBC) for financial support.

## References

- 1 C. D. Geddes, *Metal-enhanced fluorescence*, Wiley, Hoboken, NJ, 2010, ch. 2010.
- 2 H. Mishra, B. L. Mali, J. Karolin, A. I. Dragan and C. D. Geddes, *Phys. Chem. Chem. Phys.*, 2013, **15**, 19538–19544.
- 3 N. S. Abadeer, M. R. Brennan, W. L. Wilson and C. J. Murphy, *ACS Nano*, 2014, **8**(8), 8392–8406.
- 4 G. Hawa, L. Sonnleitner, A. Missbichler, A. Prinz, G. Bauer and C. Mauracher, *Anal. Biochem.*, 2018, **549**, 39–44.
- 5 L. Kong, J. Zhu, W. Wang, L. Jin, Y. Fu, B. Duan and L. Tan, *Spectrochim. Acta, Part A*, 2017, **173**, 675–680.
- 6 Q. Xie, X. Weng, L. Lu, Z. Lin, X. Xu and C. Fu, *Biosens. Bioelectron.*, 2016, **77**, 46–50.
- 7 M. G. Warner, J. W. Grate, A. Tyler, R. M. Ozanich, K. D. Miller, J. Lou, J. D. Marks and C. J. Bruckner-Lea, *Biosens. Bioelectron.*, 2009, **25**, 179–184.
- 8 A. I. Dragan, R. Pavlovic and C. D. Geddes, *Biophys. J.*, 2011, **100**, 137a–138a.
- 9 A. I. Dragan, M. T. Albrecht, R. Pavlovic, A. M. Keane-Myers and C. D. Geddes, *Anal. Biochem.*, 2012, **425**, 54–61.
- 10 A. I. Dragan, E. S. Bishop, J. R. Casas-Finet, R. J. Strouse, M. A. Schenerman and C. D. Geddes, *J. Immunol. Methods*, 2010, **362**, 95–100.
- 11 M. Bauch, K. Toma, M. Toma, Q. W. Zhang and J. Dostalek, *Plasmonics*, 2014, **9**, 781–799.
- 12 Y. Jeong, Y.-M. Kook, K. Lee and W.-G. Koh, *Biosens. Bioelectron.*, 2018, **111**, 102–116.
- 13 A. I. Dragan, B. Mali and C. D. Geddes, *Chem. Phys. Lett.*, 2013, **556**, 168–172.

- 14 C. D. Geddes, *J. Phys. Chem. C*, 2009, **113**, 12095–12100.
- 15 T. Felicia, P. G. Glenn, R. J. Bruce and J. H. Naomi, *Nano Lett.*, 2007, **7**, 496–501.
- 16 H. Ben Hamo, A. Kushmaro, R. Marks, J. Karolin, B. Mali and C. D. Geddes, *Appl. Phys. Lett.*, 2015, **106**, 081605.
- 17 J. Karonlin and C. D. Geddes, *Appl. Phys. Lett.*, 2014, **105**, 063102.
- 18 J. Asselin, P. Legros, A. Grégoire and D. Boudreau, *Plasmonics*, 2016, **11**, 1369–1376.
- 19 J. L. Yang, S. H. Cao, Q. Liu, S. Zhao, Y. B. Zheng and Y. Q. Li, *New J. Chem.*, 2015, **39**, 77–80.
- 20 B. Jose, R. Steffen, U. Neugebauer, E. Sheridan, R. Marthi, R. Forster and T. Keyes, *Phys. Chem. Chem. Phys.*, 2009, **11**, 10923–10933.
- 21 M. Diwekar, S. Blair and M. Davis, *J. Nanophotonics*, 2010, **4**, 043504–043515.